

Targeted Inhibition of Inducible Nitric Oxide Synthase Inhibits Growth of Human Melanoma *In vivo* and Synergizes with Chemotherapy

Andrew G. Sikora^{1,2,6}, Alexander Gelbard^{1,2,5}, Michael A. Davies^{1,4}, Daisuke Sano², Suhendan Ekmekcioglu³, John Kwon³, Yared Hailemichael¹, Padmini Jayaraman⁶, Jeffrey N. Myers², Elizabeth A. Grimm³, and Willem W. Overwijk¹

Abstract

Purpose: Aberrant expression of inflammatory molecules, such as inducible nitric oxide (NO) synthase (iNOS), has been linked to cancer, suggesting that their inhibition is a rational therapeutic approach. Whereas iNOS expression in melanoma and other cancers is associated with poor clinical prognosis, *in vitro* and *in vivo* studies suggest that iNOS and NO can have both protumor and antitumor effects. We tested the hypothesis that targeted iNOS inhibition would interfere with human melanoma growth and survival *in vivo* in a preclinical model.

Experimental Design: We used an immunodeficient non-obese diabetic/severe combined immunodeficient xenograft model to test the susceptibility of two different human melanoma lines to the orally-given iNOS-selective small molecule antagonist N⁶-(1-iminoethyl)-L-lysine-dihydrochloride (L-nil) with and without cytotoxic cisplatin chemotherapy.

Results: L-nil significantly inhibited melanoma growth and extended the survival of tumor-bearing mice. L-nil treatment decreased the density of CD31+ microvessels and increased the number of apoptotic cells in tumor xenografts. Proteomic analysis of melanoma xenografts with reverse-phase protein array identified alterations in the expression of multiple cell signaling and survival genes after L-nil treatment. The canonical antiapoptotic protein Bcl-2 was downregulated *in vivo* and *in vitro* after L-nil treatment, which was associated with increased susceptibility to cisplatin-mediated tumor death. Consistent with this observation, combination therapy with L-nil plus cisplatin *in vivo* was more effective than either drug alone, without increased toxicity.

Conclusions: These data support the hypothesis that iNOS and iNOS-derived NO support tumor growth *in vivo* and provide convincing preclinical validation of targeted iNOS inhibition as therapy for solid tumors. *Clin Cancer Res*; 16(6); 1834–44. ©2010 AACR.

Authors' Affiliations: Departments of ¹Melanoma Medical Oncology, ²Head and Neck Surgery, ³Experimental Therapeutics, and ⁴Systems Biology, University of Texas M.D. Anderson Cancer Center; ⁵Bobby Alford Department of Otolaryngology, Baylor College of Medicine, Houston, Texas and ⁶Departments of Otolaryngology, Immunobiology, Oncological Sciences, and Dermatology, Mount Sinai School of Medicine, New York, New York

Note: Supplementary data for this article are available at Clinical Cancer Research Online (<http://clincancerres.aacrjournals.org/>).

A.G. Sikora and A. Gelbard contributed equally to the work described in this manuscript.

Corresponding Author: Willem W. Overwijk, Department of Melanoma Medical Oncology, University of Texas M.D. Anderson Cancer Center, 1515 Holcombe Boulevard, Unit 430, Houston, TX 77030. Phone: 713-563-5294; Fax: 713-563-3424; E-mail: woverwijk@mdanderson.org or Andrew G. Sikora, Mount Sinai School of Medicine, One Gustave L. Levy Place, Box 1189, New York, NY 10029. Phone: 212-659-9516; Fax: 212-369-5701; E-mail: andrew.sikora@mssm.edu.

doi: 10.1158/1078-0432.CCR-09-3123

©2010 American Association for Cancer Research.

Upregulation of proinflammatory molecules by tumor cells is a poorly understood phenomenon, which can play a role in both the induction and maintenance of certain human cancers (1). One such molecule, inducible nitric oxide (NO) synthase (iNOS) is constitutively overexpressed in many cancers, including melanoma and gastric (2), breast (3), colon (4), and head and neck (5, 6) carcinomas. iNOS and its product NO have wide-ranging and varied effects on cellular physiology, signal transduction, and cell survival. At high levels, such as produced by activated macrophages during inflammatory responses to pathogens, NO alone or in combination with reactive oxygen species can have a direct cytotoxic effect on pathogens or tumor cells (7). At lower levels, NO can affect signal transduction pathways by interacting with metal ligands of proteins (8) or covalently modifying proteins through nitration and nitrosylation (9, 10). These protein

Translational Relevance

Currently there is no reliably effective "standard of care" treatment for advanced melanoma. In this study, we show that the small molecule inducible nitric oxide synthase inhibitor N⁶-(1-iminoethyl)-L-lysine-dihydrochloride has potent antimelanoma activity and can be effectively used in combination with cytotoxic chemotherapy *in vivo*. Because N⁶-(1-iminoethyl)-L-lysine-dihydrochloride and related drugs have previously been used in noncancer human studies, targeted inducible nitric oxide synthase inhibition has great potential for translation to clinical trials for melanoma and other solid tumors.

modifications can increase or decrease enzyme activity or enhance protein stability depending on the specific amino acid residues modified, the amount of available NO, the redox status of the cell, and the availability of protein substrates (9, 10). As NO can modulate numerous signal transduction pathways in cancer cells via posttranslational protein modification, iNOS expression can potentially serve as a global regulator of carcinogenesis and tumor behavior.

A link between iNOS and cancer development and progression has been proposed based on both clinical and experimental evidence. On balance, data from *in vivo* tumor models and cell culture studies support a link between iNOS/NO and carcinogenesis, tumor progression, tumor survival, and aggressiveness (reviewed in refs. 11–13), but results vary greatly depending on the experimental model used. *In vitro*, low-level NO production, such as that produced by many human tumor cells, seems to support tumor growth and survival by a variety of mechanisms, including enhancing the stability of the antiapoptotic protein Bcl-2 via S-nitrosylation (14) and inhibiting the proapoptotic activity of caspase-3 (15). In both *in vitro* and *in vivo* models, iNOS and NO have been variously shown to enhance carcinogenesis and tumor progression, stimulate angiogenesis, support tumor growth, promote metastasis, and inhibit T cell–dependent immune responses (reviewed in refs. 11, 13, 16). Thus there is substantial interest in iNOS and NO as therapeutic targets for cancer therapy.

Malignant melanoma is among the fastest-growing causes of cancer death, responsible for roughly 68,720 new cases and 8,650 deaths in the United States in 2009 (17). Whereas early-stage disease is generally treatable by surgery, there is no consistently effective treatment for metastatic disease. In melanoma, iNOS expression is absent in benign nevi and present in invasive melanoma (18), and the level of expression correlates strongly with poor clinical outcome (19, 20). *In vitro* data support the ability of NO to protect human melanoma cells from apoptosis, and NO depletion enhances sensitivity to cisplatin (21).

Thus, both clinical and *in vitro* evidence supports the hypothesis that targeted inhibition of iNOS and iNOS-derived NO may be an effective therapeutic approach for melanoma and other iNOS-expressing tumors.

In the present study, we tested the effect of iNOS inhibition with small-molecule antagonists on human melanoma *in vivo* using a xenograft model. We found that the iNOS selective antagonist N⁶-(1-iminoethyl)-L-lysine dihydrochloride (L-nil; ref. 22) inhibited iNOS-dependent NO production by human melanoma cells in a dose-dependent fashion *in vitro* and strongly suppressed melanoma growth *in vivo* without evident toxicity. Growth suppression was associated with a decrease in tumor microvessels, downregulation of the antiapoptotic gene Bcl-2, increased number of intratumoral apoptotic cells, and enhanced efficacy when L-nil treatment was combined with cisplatin *in vivo*. These data suggest that iNOS-selective small molecule inhibitors, alone or in combination with conventional cytotoxic chemotherapy, are a promising approach to therapy of melanoma and other solid tumors.

Materials and Methods

Western blots. Cell lysates were separated by size using SDS-PAGE and transferred to a membrane. Membranes were incubated with a primary antibody against iNOS (sc-651, Santa Cruz Biotech), Bcl-2 (PharMingen), or extracellular signal-regulated kinase 2 (sc-154, Santa Cruz) followed by a secondary antibody conjugated to horseradish peroxidase. Relative signal intensities for Bcl-2 were validated by Western blot, and normalized densitometry values were expressed as ratio of Bcl-2 to extracellular signal-regulated kinase 2 protein levels.

Tumor cell lines and transient transfection. The human melanoma cell lines mel624 and mel528 were a kind gift from Dr. J. Wunderlich, Surgery Branch, National Cancer Institute, NIH. The A375 human melanoma line was purchased from American Type Culture Collection. The human colon line WiDR was a kind gift of J. Hodge, Laboratory of Tumor Immunology and Biology, National Cancer Institute, NIH. WiDR cells were transfected with Lipofectamine according to the manufacturer's (Invitrogen) protocol. At 24 h after transfection, cells were replated for use in the indicated assays. Plasmid expressing the gene encoding full-length human iNOS protein was a generous gift from Keping Xie and has been previously described (23). All melanoma lines were submitted to the Characterized Cell Line Core of the M.D. Anderson Cancer Center Support Grant.⁷ Fingerprinting analysis is done, and cells are validated every 2 y; the lines in this study were validated in March 2008.

Detection of NO and *in vitro* inhibitor experiments. Cell lines were cultured in phenol-free DMEM supplemented

⁷ <http://inside.mdanderson.org/departments/ccsg/characterized-cell-line-core/charcell.html>

with 10% fetal bovine serum, penicillin, and streptomycin at 37°C in 5% CO₂. Cells (2×10^5) were cultured in a 24-well plate with the indicated concentration of L-NIL for 72 h before assay for cell death or NO levels. Cumulative NO production was measured *in vitro* by the nitrite reconversion method with the Apollo 4000 bioanalyzer (World Precision Instruments) as previously described (24). In cytotoxicity experiments, the 2,3-bis[2-methoxy-4-nitro-5-sulfophenyl]-2H-tetrazolium-5-carboxanilide inner salt (XTT) cell proliferation assay (Cayman Chemical) or Annexin/propidium iodide cell death assay (BD Biosciences) was used according to the manufacturer's directions.

For *in vivo* NO measurements, C57BL/6 mice received 0.1% L-nil in drinking water or plain water control for 48 h before i.p. injection of 250 µg lipopolysaccharide (LPS). Mice were sacrificed at 7 h postinjection, and serum was prepared from whole blood by centrifugation. Serum was then clarified by passage through a 10-kDa cutoff spin-filter (Millipore), and nitrite levels were determined by Griess assay (25).

L-nil was obtained from A.G. Scientific. Griess reagent, 1,3-PBIT, LPS, and aminoguanidine were obtained from Sigma Aldrich Corp.

Intracellular Bcl-2 staining. Staining with anti-Bcl-2 antibody was modified from the published protocol (26). In brief, cells were permeabilized using cytofix/cytoperm kit (BD Pharmingen) and stained with Bcl-2-FITC antibody or matched isotype control (BD Pharmingen).

Animals and in vivo tumor experiments. Female non-obese diabetic (NOD)/severe combined immunodeficient (SCID) mice (ages 6–8 wk) were purchased from the Animal Production Area of the National Cancer Institute-Frederick Cancer Research and Development Center. Female C57BL/6 mice (ages 6–8 wk) were purchased from JAX labs. The mice were bred and maintained in a pathogen-free environment and fed irradiated mouse chow and autoclaved reverse osmosis-treated water. All of the animal procedures were done in accordance with a protocol approved by the Institutional Animal Care and Use Committee of the University of Texas M.D. Anderson Cancer Center. In xenograft experiments, animals were injected with human melanoma tumor cell lines (either mel624 or A375) at initial concentrations of 5×10^6 or 7.5×10^6 in 100 µL PBS, respectively. Animals were randomized after tumors established and assigned to experimental groups (10 per group unless otherwise noted). Experimental animals received 0.15% or 0.2% L-NIL or 0.2% PBIT in their drinking water, replaced every 2 to 3 d, beginning 3 d after tumor implantation. Control animals received plain drinking water. In some experiments, animals received cisplatin given at the indicated dose and time point via i.p. injection. Animals were weighed regularly and monitored for signs of toxicity. Tumor growth was measured thrice per week using electronic calipers, and tumor volumes were determined by multiplying the longest axis by its perpendicular. Mice were humanely sacrificed when tumors reached >250 mm², ulceration occurred, or mice become moribund.

In some tumor experiments, representative animals were evaluated by magnetic resonance imaging (MRI) using a 7.0T Biospec USR small animal imaging system (Bruker Biospin MRI). A linear volume resonator with 35 mm inner diameter was used for signal excitation and detection. Axial T1-weighted (TE/TR 8.5 ms/900 ms, two averages, 156 nm × 156 nm × 1 mm resolution) and T2-weighted images (TE/TR 65 ms/5,000 ms, RARE factor 12, three averages) with matching slice prescriptions were collected for tumor visualization.

Immunohistochemistry. Paraffin-embedded sections of excised human melanoma tumor xenografts were examined for nitrotyrosine and iNOS expression by immunohistochemistry using an anti-nitrotyrosine polyclonal antibody (Upstate Biotechnology) or anti-iNOS monoclonal antibody (BD-Transduction Laboratories). Preimmune normal rabbit IgG (Vector Laboratories) and anti-vimentin antibody (BioGenex Laboratories) were used as negative and positive controls, respectively. Tissue sections were deparaffinized and rehydrated, then placed in Antigen Unmasking Solution (Vector Laboratories), and microwaved intermittently for a total of 10 min to maintain boiling temperature. After cooling, the slides were placed in 3% H₂O₂ in cold methanol for 15 min and then 0.05% Triton X-100 (Sigma) for 15 min. An avidin-biotin-peroxidase complex kit (Vectastain, Vector Laboratories) was then used for antigen detection according to the manufacturer's instructions, and immunolabeling was developed with the chromogen 3-amino-9-ethylcarbazole for 10 min.

For detection of CD31, frozen tumor sections were fixed in cold acetone for 10 min before immunostaining with anti-CD31 primary antibody (Pharmingen) for 1 h at room temperature, detection with peroxidase-conjugated secondary antibody, and counterstaining with hematoxylin. Terminal deoxynucleotidyl transferase-mediated dUTP nick end labeling (TUNEL) assay was done on paraformaldehyde-fixed tissues with an apoptosis detection kit (Promega) according to the manufacturer's direction. CD31/TUNEL double-staining was done by subjecting the same tissues to sequential CD31 immunostaining with Alexa Fluor 594-conjugated secondary antibody and TUNEL assay with fluorescein-dUTP.

Quantification of nitrotyrosine, iNOS, microvessel density, apoptotic tumor, mean vessel diameter, and endothelial cells. Immunofluorescence microscopy images were obtained with a Leica DMLA microscope (Leica Microsystems) equipped with a Hamamatsu 5810 cooled CCD camera (Hamamatsu Corp.) and ImagePro Plus 6.0 software (Media Cybernetics). Photomontages were prepared using Adobe Photoshop software (Adobe Systems, Inc.). For the quantification analysis, four slides were prepared for each group. The percentage of positively-staining cells in each group was calculated and compared. For quantification of TUNEL expression, the cells positively stained were counted in five random 0.04-mm² fields at 200× magnification per slide. To quantify microvessel density, areas containing higher numbers of tumor-associated blood vessels were identified at low microscopic power (100×).

Vessels completely stained with anti-CD31 antibodies were counted in five random 0.159-mm² fields at 100× magnification per slide. For comparison of vessel diameter between control and experimental groups, mean diameter in pixels was calculated for the stained blood vessels in 10 random 0.159-mm² fields at 100× magnification.

Reverse-phase protein array. Reverse-phase protein array (RPPA) as done has been described previously (27) and was used to quantify protein and phosphorylated protein expression of 59 cancer-related and signal transduction proteins, including Bcl-2, phosphorylated PDK1 (Ser²⁴¹), phosphorylated AMPK (Thr¹⁷²), 4EBP1, P70S6K, S6, TSC2, PTEN, mammalian target of rapamycin (mTOR), and others. Comparison antibodies were from Cell Signaling (PTEN, mTOR, and all phosphorylated-specific antibodies), Epitomics, Inc. (total p70S6K antibody), and DAKO (Bcl-2).

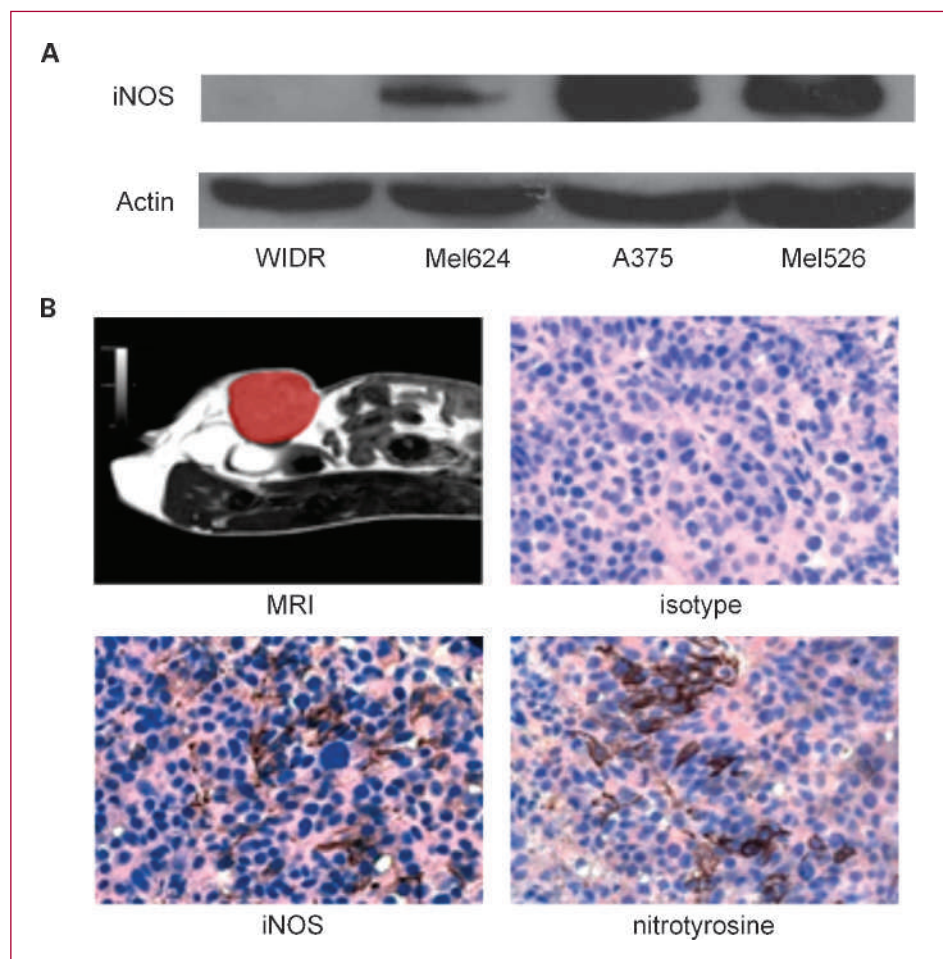
Statistical analysis. The quantifications of the immunohistochemical expression of nitrotyrosine, iNOS, TUNEL, microvessel density, and mean vessel diameter were compared by the paired Student's *t* test, with significance at *P* < 0.01. For *in vitro* experiments, Student's *t* test and a significance threshold of *P* < 0.05 was used. For *in vivo* survival

experiments, Kaplan-Meier survival curves were generated, and significant differences were determined using the log-rank test. *In vivo* tumor growth curves were compared using the nonparametric method of Koziol et al. to allow comparisons despite unequal survival of mice between groups (28).

Results

Human melanoma lines express iNOS and release NO, which is inhibited by the selective antagonist L-nil. Western blot analysis was used to screen melanoma cell lines for iNOS protein expression (Fig. 1A), using the previously confirmed iNOS-negative colon cancer cell line WiDR (4) as a negative control. iNOS protein was strongly expressed in the melanoma lines mel526 and A375 and expressed less strongly in mel624. iNOS expression was maintained *in vivo*, as A375 tumor xenografts were strongly positive for both iNOS and the stable NO end product nitrotyrosine by immunohistochemistry (Fig. 1B). The presence of nitrotyrosine shows that iNOS is expressed and catalyzes NO production in human melanoma cells.

Fig. 1. Human melanoma lines constitutively express iNOS and make NO *in vitro* and *in vivo*. A, human melanoma lines mel624, A375, and mel526 and the iNOS-negative colon cancer line WiDR were assessed by Western blot for iNOS protein expression. B, 5×10^6 A375 melanoma cells were injected s.c. into recipient NOD/SCID mice and allowed to form 0.5-cm tumors. Xenografts were then harvested, and sections were stained by immunohistochemistry for iNOS and the stable NO reaction product nitrotyrosine. Representative MRI (tumor in false color) and immunohistochemistry results.



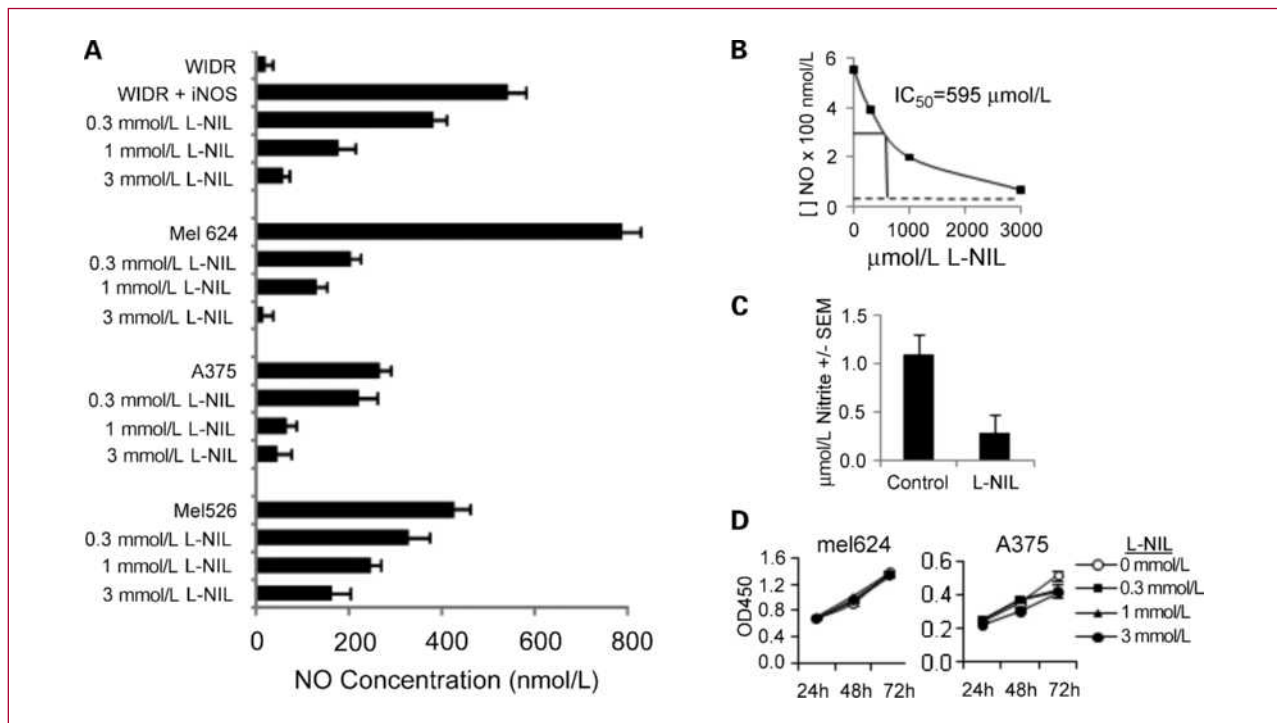


Fig. 2. The iNOS-selective competitive antagonist L-nil blocks iNOS-derived NO production *in vitro* and *in vivo* without affecting cell viability. A, human melanoma lines mel624, A375, and mel526 or colon cancer line WIDR or WIDR transfected with iNOS plasmid were incubated for 72 h with the indicated concentrations of L-nil and NO released into the supernatant, measured using the nitrite reconversion method. B, the effect of L-nil on NO production by WIDR + iNOS plasmid was used to determine the IC₅₀ of L-nil in the cell culture system. C, serum was collected 7 h after i.p. LPS injection of C57BL/6 mice (four per group) pretreated for 48 h with 0.1% L-nil in drinking water (L-nil) or plain drinking water (control). Nitrite levels were determined using the Griess assay. D, Mel624 or A375 melanoma cells were cultured for the indicated length of time in medium containing varying concentrations of L-nil, and proliferation was measured by XTT assay.

As basal NO production by melanoma lines was consistently at the lower limit of detection of the relatively insensitive Griess assay, further NO measurements were made with the TBI 4100 electrochemical NO probe (WPI Instruments), which is capable of measuring nanomolar levels of NO. All iNOS-positive melanoma lines produced nanomolar levels of NO (Fig. 2A). Basal NO levels in media from WIDR cells (which do not express iNOS mRNA; ref. 29) were just above those of medium alone; after transfection with an iNOS-encoding expression plasmid, WIDR/iNOS cells released NO at levels comparable with melanoma cells. The iNOS-selective competitive antagonist L-nil, when added to culture medium, inhibited NO release by WIDR/iNOS and melanoma cells in a dose-dependent fashion. The IC₅₀, calculated from WIDR/iNOS cells (for which the only significant source of measurable NO is exogenously-supplied iNOS), was 595 μmol/L (Fig. 2B). The decrease in NO production by L-nil was not due to cytotoxicity, as viability of melanoma cells was not significantly affected by L-nil after up to 72 hours incubation (Fig. 2D).

To test whether L-nil could reach a biologically relevant and therapeutic concentration *in vivo*, C57BL/6 mice received L-nil (0.15%) in drinking water before i.p. challenge with LPS, a strong inducer of iNOS-dependent NO production from resident macrophages. L-nil treatment re-

sulted in a strong decrease in serum nitrite levels after LPS challenge (Fig. 2C), showing the ability of orally given L-nil to inhibit iNOS activity *in vivo*.

Targeted inhibition of iNOS antagonizes human melanoma growth *in vivo* and extends survival of tumor-bearing mice. We provided L-nil (0.15% in drinking water) or plain drinking water control to NOD/SCID mice bearing mel624 xenografts beginning on day 3 after tumor implantation. L-nil suppressed tumor growth for as long as the inhibitor was supplied in drinking water (4 weeks; Fig. 3A). Whereas the tumor resumed growth after discontinuation of treatment, L-nil-treated mice survived significantly longer than untreated mice (Fig. 3B). Another iNOS antagonist, 1,3-PBIT, had a similar effect on mel624 growth when given in drinking water (Fig. 3C), suggesting that the antitumor effect of L-nil is due to iNOS inhibition rather than non-specific cytotoxicity or activity against non-NOS targets. Neither L-nil nor 1,3-PBIT caused any outward signs of toxicity in mice (behavioral changes, reduction in food or water intake, ruffled fur, hunched posture) after 4 weeks at the indicated concentration. There was no significant difference in body weight among control, L-nil, and 1,3-PBIT groups (Fig. 3D) at the indicated doses; however, wasting and behavioral changes were seen at higher doses of 1,3-PBIT.

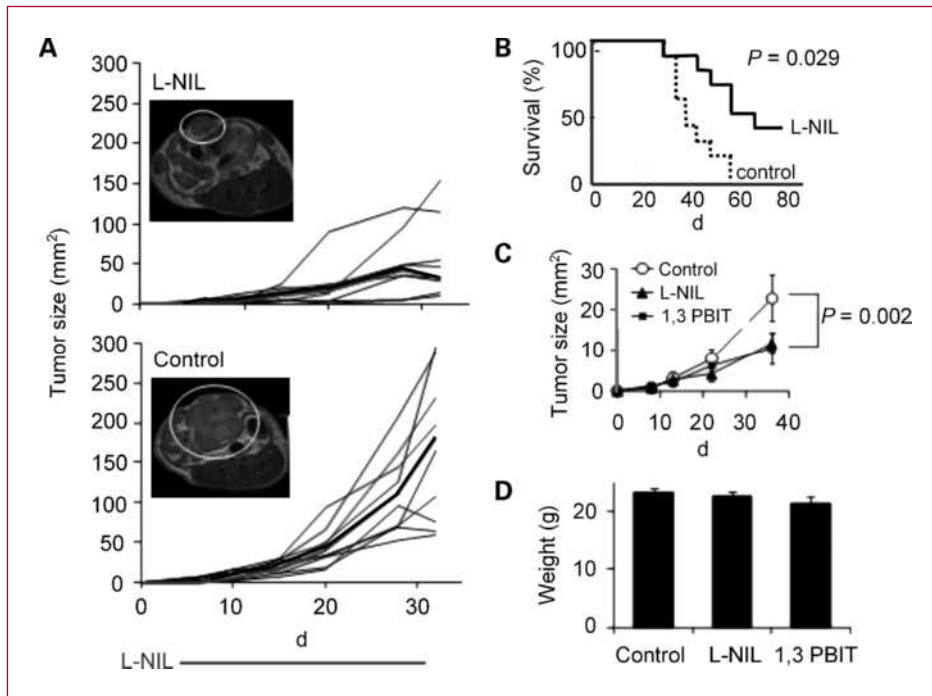


Fig. 3. Orally delivered selective iNOS antagonists suppress the growth of human melanoma and extend survival without overt toxicity in an immunodeficient mouse xenograft model. A, 5×10^6 mel624 cells were injected s.c. on day 0. Starting on day 3, mice were treated with 0.15% L-nil in drinking water or plain water control for 28 d. Tumor sizes are expressed as mm^2 ; each black line represents an individual mouse; median size is with a bold line. Inset, representative MRI pictures of day 22 tumors from L-nil-treated (top) and control-treated (bottom) mice. Data are representative of three experiments. B, Kaplan-Meier survival estimates for control-treated and 0.15% L-nil-treated mel624-bearing mice. C, using the experimental design described in A, mel624-bearing mice were treated with 0.15% L-nil or 0.2% 1,3-PBIT in drinking water or plain drinking water control for 28 d starting on day 3. Tumor sizes are expressed as mean \pm SEM. Data are representative of two experiments. D, mice were weighed after 21 d treatment with 0.15% L-nil or 0.2% PBIT in drinking water or plain water control.

iNOS inhibition results in decreased intratumoral microvessel density, downregulation of Bcl-2, and increased intratumoral apoptosis in vivo. As expected, treatment with L-nil did not appreciably alter *in vivo* expression of iNOS protein levels in melanoma xenografts, but reduced staining for nitrotyrosine confirmed the inhibition of intratumoral NO levels (Fig. 4). Because NO is known to have angiogenic activity via induction of vascular endothelial growth factor expression, we examined microvessel density in mel624 xenografts by immunohistochemistry for the vascular endothelial marker CD31 (Fig. 4). After 19 days of L-nil treatment, there was a significant ($P = 0.006$) decrease in density of CD31+ microvessels in L-nil-treated mice, although the vessels' diameter was significantly greater (insert; average of 27 ± 2 pixels versus 10 ± 1 pixels in diameter). Because NO has been suggested to inhibit apoptosis in human melanoma cells *in vitro* (21), we next examined the density of apoptotic (TUNEL+) cells in xenografts from L-nil-treated and control-treated mice (Fig. 5A). Tumors from L-nil-treated mice contained ~3-fold more TUNEL+ cells than tumors from control mice, suggesting that the decreased growth of xenografts is at least in part due to a higher rate of cell death. Staining of serial sections with TUNEL and the vascular marker CD31 did not reveal consistent colocalization of TUNEL

staining and CD31 (Fig. 5A), as would be expected if endothelial cells were undergoing frequent apoptosis. Distribution of apoptotic cells was also not restricted to areas lacking vessel growth.

To further explore the possible mechanisms of tumor inhibition by L-nil, we measured the protein and phosphorylated protein expression of 59 proteins involved in signal transduction and cell survival pathways by RPPAs (Supplementary Table S1). Two tumors were analyzed for each treatment, and multiple samples from each tumor were analyzed to control for intratumoral heterogeneity. This analysis showed consistent decreases in multiple proteins, including several components of the phosphoinositide 3-kinase/AKT signaling pathway, although we did not observe changes in phosphorylated AKT itself (Supplementary Fig. S1). A potential link between iNOS inhibition and increased apoptosis in tumors from L-nil-treated mice was suggested by a marked decrease in Bcl-2 expression levels, which was confirmed by Western blotting analysis (Fig. 5B). Bcl-2 is not only a critical regulator of cell death in response to a variety of stimuli, but its posttranslational stability is also known to be regulated by NO via nitrosylation of key cysteine residues (14). This mechanism is supported by the observation that prolonged treatment of A375 melanoma cells

with 1 mmol/L L-nit almost completely abolished Bcl-2 expression (Fig. 5C).

Combination therapy with cisplatin + L-nit is effective against human melanoma cell lines *in vivo*. NO is known to affect signal transduction pathways regulating apoptosis (Bcl-2, caspase III, p53, and other survival and death pathways), and depletion of NO with the chemical NO scavenger PTIO has been shown to enhance sensitivity of human melanoma cells to cisplatin *in vitro* (21). Because we found that L-nit downregulated Bcl-2 expression in melanoma cells *in vivo*, we hypothesized that L-nit treatment would potentiate cytotoxic therapy of melanoma. Because resis-

tance to conventional cytotoxic agents is a common clinical problem, we used both a relatively cisplatin-sensitive human melanoma line (A375) and the line mel624, which is 3-fold to 4-fold more resistant to cisplatin (Fig. 6A). Whereas neither cell line was sensitive to L-nit treatment alone (Fig. 2C) *in vitro*, pretreatment of A375 cells with L-nit for 5 days increased sensitivity of cells to cisplatin-induced killing (Fig. 6B).

We then tested combination therapy with L-nit plus cisplatin against human melanoma *in vivo*. Whereas cisplatin or L-nit alone only partially suppressed the growth of established mel624 and A375, combination therapy with L-nit and cisplatin inhibited growth of mel624 and A375 more efficiently than either drug alone (Fig. 6C) without additional toxicity. Although mice received only a single three-dose course of cisplatin treatment, continued treatment with L-nit alone was sufficient to suppress tumor growth.

Discussion

Whereas inflammation plays a well-established role in the initiation and progression of certain cancers, the ability of proinflammatory molecules to support the persistence of established cancer is a relatively recent observation. The present data confirm the hypothesis that iNOS is one such inflammatory mediator capable of promoting the survival and proliferation of human melanoma cells *in vivo*. More importantly, we show that iNOS can be readily targeted in melanoma without overt toxicity and that iNOS inhibition reverses the chemoresistance of human melanoma.

Our data are consistent with previous studies, mostly *in vitro*, which show an effect of NOS inhibition on tumor growth, survival, or both (30–33). Our study is among the first to show dramatic antitumor activity of iNOS-selective inhibitors *in vivo* and feasibility of combination treatment of cancer combining targeted iNOS inhibition and cytotoxic chemotherapy. There are several potential mechanisms by which iNOS antagonists may inhibit tumor growth, either directly or by sensitizing cells to other forms of stress, such as hypoxia or reactive oxygen species-mediated stress. Mechanisms by which iNOS inhibition may affect the resistance of cancer cells to apoptosis include interference with phosphoinositide 3-kinase/AKT-mediated overexpression of survivin (34, 35) or reversal of caspase inactivation (15) or Bcl-2 stabilization mediated by S-nitrosylation of these proteins (14). Indeed, we observed that L-nit induced downregulation of Bcl-2 protein expression *in vivo* and *in vitro*, suggesting that this is one mechanism by which iNOS inhibition may enhance susceptibility of cancer cells to apoptosis. L-nit's relative lack of direct cytotoxicity *in vitro* (Fig. 2C), despite causing markedly increased tumor apoptosis *in vivo*, may reflect the relative absence of stressful stimuli (hypoxia, acidosis, cytokines, etc.) *in vitro*, which might force melanoma cells to depend on Bcl-2 expression for survival.

NO has well-established proangiogenic properties, and stimulation of angiogenesis is one proposed mechanism

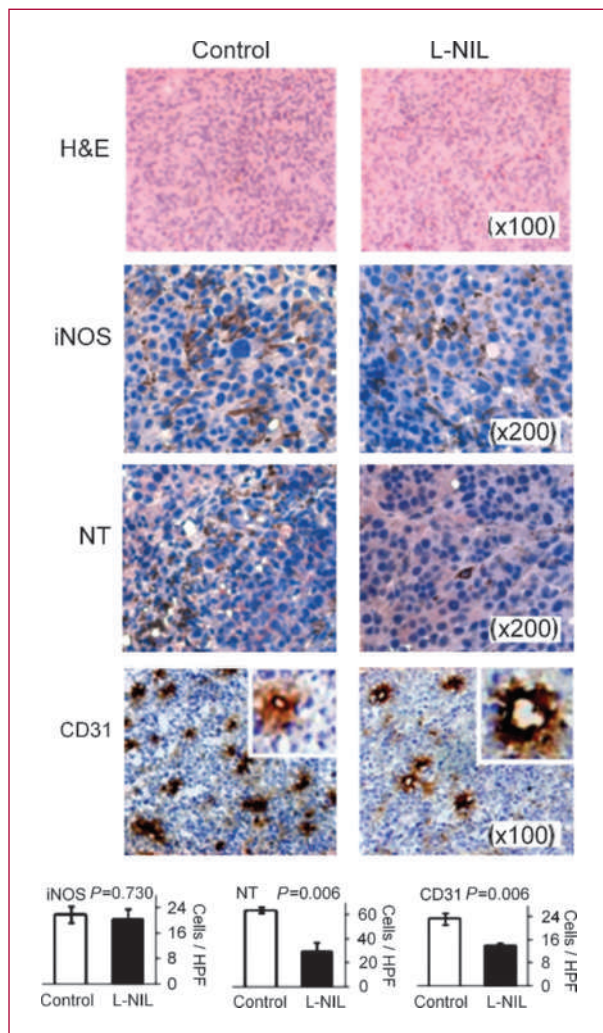


Fig. 4. Oral L-nit treatment inhibits intratumoral nitrotyrosine formation and decreases tumor microvessel density. Mel624-bearing mice were treated for 14 d with 0.15% L-nit in drinking water or plain water control before sacrifice, harvest of xenografts, and H&E staining (top) or immunohistochemical staining for iNOS, nitrotyrosine (NT), or the vascular marker CD31. Representative images are shown at the indicated original magnifications, except the insert pictures of representative CD31-stained vessels at 400 \times . Computer-assisted quantitation of images is shown below.

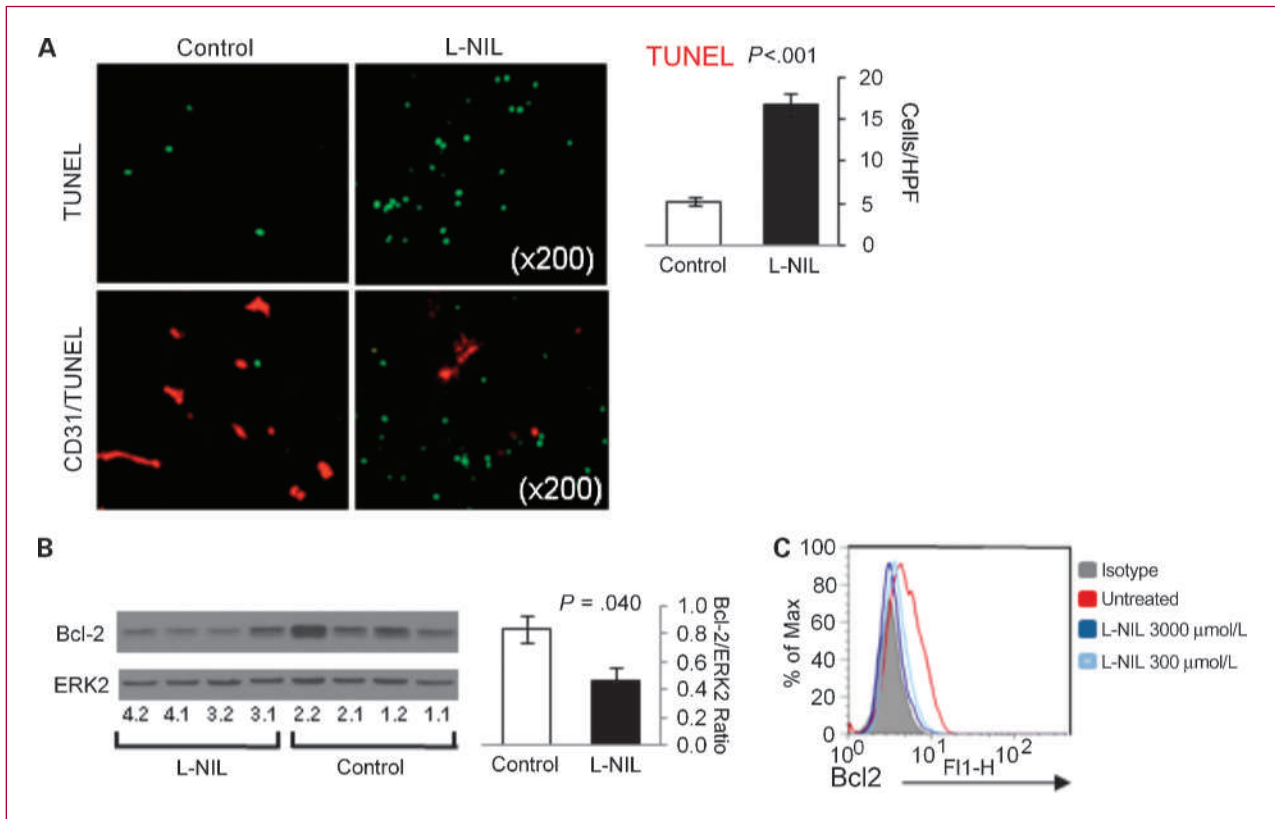


Fig. 5. L-nil downregulates Bcl-2 expression and induces intratumoral apoptosis *in vivo*. **A**, Mel624 xenografts were harvested from mice after treatment with 0.15% L-nil or plain water control for 14 d. Paraffin-embedded slides were subjected to TUNEL analysis of apoptotic cells (top) or double-staining for TUNEL and the vascular marker CD31 (bottom). Representative images are shown on the left and quantitation of TUNEL staining on the right. **B**, Western blot analysis mel624 xenograft lysates was done to confirm downregulation of Bcl-2 expression in tumors from L-nil-treated mice (two replicates of two tumors per group). The bar graph shows quantitation of Bcl-2 levels (normalized to Erk2 protein expression) in tumors from control and L-nil-treated mice. **C**, 5×10^4 A375 cells were cultured in 48-well plates for 3 d with the indicated concentration of L-nil, at which time the medium and inhibitor were replenished and cells were cultured for an additional 2 d before immunostaining for intracellular Bcl-2 and analysis by flow cytometry.

by which iNOS expression may support tumor growth (36, 37). We observed a nearly 2-fold decrease in tumor microvessel density in tumors from L-nil-treated mice, although the average caliber of the remaining vessels was greater (see inset, Fig. 4, bottom). As both suppression of vascularization and increased apoptosis may lead to a diminished overall rate of tumor growth, they may act additively or synergistically to cause the observed significant decrease in tumor growth *in vivo*.

Another potential mechanism of tumor growth suppression is interference with the NO-dependent proliferation of tumor cells. Whereas relatively few studies have attempted to disentangle the dual effect of NO on tumor cell survival and proliferation, NO has been shown to increase proliferation of human breast cancer cells *in vitro* via stimulation of the AKT/mTOR pathway and downstream upregulation of cyclin D1 (38). It is interesting that, of the nearly 60 proteins and phosphorylated proteins we examined by RPPA, multiple proteins in the mTOR pathway, including P70S6K, and mTOR were significantly and coordinately downregulated by L-nil treatment *in vivo* (Supplementary Fig. S1). We are currently investigating the effect

of iNOS/NO inhibition on melanoma proliferation and regulation of the AKT/mTOR and other proliferation/survival pathways.

When we tested the *in vivo* antitumor efficacy of iNOS inhibition, alone and in combination with cisplatin, both lines tested exhibited nearly complete sensitivity to combination treatment with doses of L-nil and cisplatin that were only partly therapeutic as single agents. Because melanoma quickly acquires resistance to conventional chemotherapy in the clinical setting, restoring the efficacy of cytotoxic chemotherapy by adding a well-tolerated targeted agent to the regimen is an exciting possibility that deserves testing in clinical trials. It is notable that although cisplatin was given for only a single three-dose course, the beneficial effect of combination therapy persisted for significantly longer, so long as L-nil was continued. This suggests the potential for therapeutic regimens, which use up-front or periodic combination chemotherapy/targeted therapy followed by maintenance therapy with a relatively nontoxic targeted iNOS inhibitor.

The use of L-nil and related compounds *in vivo* seems promising because of the magnitude of tumor inhibition

(by a factor of 3-fold to 5-fold at 4 weeks) and its favorable toxicity profile. Whereas it important to note that we did not monitor changes in blood pressure, a potential side effect of chronic treatment with NO active compounds, we did not observe any overt L-nil toxicity at doses of up to 0.2% (7.7 mmol/L in drinking water) when given for up to 4 weeks. This is despite our observation that L-nil is a relatively weak inhibitor *in vitro*, with an IC_{50} of nearly 600 $\mu\text{mol/L}$ (Fig. 2A and B). This is significantly higher than the published IC_{50} values for L-nil in cell-free enzyme assays (22) and likely reflects the need for active transport of the molecule across the cell membrane (39) as well as degradation in aqueous solution over the course of 24-hour culture (Cayman Chemical product information). Variations in the efficiency of transport may also contribute to differences in the efficacy of L-nil-mediated NO suppression among our panel of cell lines. In our *in vitro* experiments, the predicted concentration of L-nil required to suppress > 90% NO production varied from 1 to >3 mmol/L. This is quite similar to the theoretical concentration of L-nil in tissues *in vivo* during treatment (assuming complete absorption of the drug in a drinking water volume of 6 mL/d), which would be 2.13 mmol/L. Because complete drug distribution into the bloodstream after oral administration is unlikely, the tumor suppressive effects observed *in vivo* are likely due to partial, rather than complete, inhibition of iNOS; this is also supported by the partial inhibition of intratumoral nitrotyrosine deposition

(Fig. 4) and LPS-induced nitrite production *in vivo* (Fig. 2D) after treatment with 0.1% L-nil. This suggests that it may be possible to more efficiently inhibit iNOS by escalating the dose of L-nil, potentially improving its antitumor efficacy. As L-nil and similar NOS inhibitors have previously been the subject of noncancer human clinical trials (40–42), these findings have strong translational potential.

Our results do not exclude the possibility that the anti-tumor activity of L-nil is enhanced by inhibition of iNOS in other (host) cell types *in vivo*. This is particularly relevant because there is little direct cytotoxic effect of L-nil *in vitro*. iNOS can be expressed by host stromal, endothelial, and bone marrow-derived cells present in tumors *in vivo*, and inhibition of NO production by any of these cell types could indirectly affect tumor growth and viability. We are currently working to determine what role, if any, host-derived iNOS plays in the antitumor effect of L-nil on melanoma xenografts *in vivo*. Another limitation of our experimental system is reliance on small molecule iNOS-selective inhibitors to implicate iNOS-derived NO in the growth and resistance to cytotoxicity of tumor cells. No chemical inhibitor is completely selective, and in fact many so-called “targeted” agents can act on a relatively broad set of molecular targets (43). However, the similar antitumor activity of two structurally dissimilar iNOS inhibitors, L-nil and 1,3 PBIT (Fig. 3C), suggests that iNOS is indeed the primary target of these treatments. Finally,

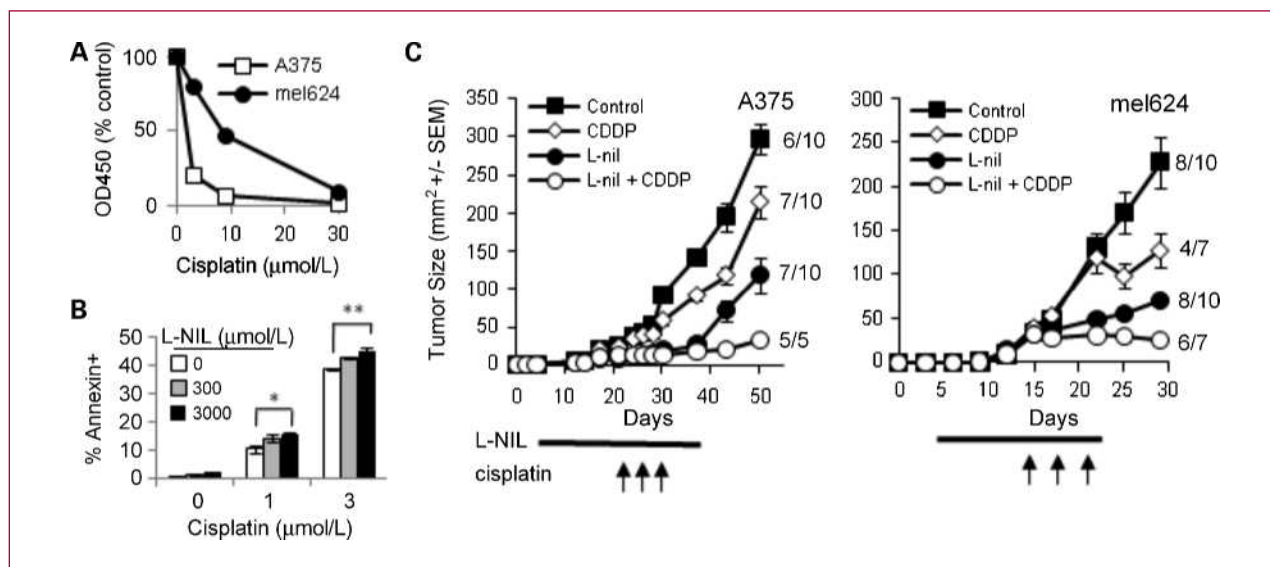


Fig. 6. L-nil enhances sensitivity of human melanoma cells to antitumor effect of cisplatin *in vitro* and *in vivo*. A, A375 and mel624 cells were treated with the indicated concentrations of cisplatin for 48 h, and proliferation was measured by XTT assay. Data are presented as mean \pm SEM and are representative of three independent experiments. B, 2×10^4 A375 melanoma cells were cultured in the indicated concentration of L-nil for 3 d. On day 3, the medium was discarded, and cells were incubated for another 48 h in fresh media with the indicated concentration of L-nil and/or cisplatin. Cells were then trypsinized, and cell death was assessed by Annexin V staining and flow cytometry. Data are presented as mean \pm SEM and are representative of three independent experiments. *, $P = 0.012$; **, $P = 0.003$. C, SCID-NOD mice were injected s.c. with 5×10^6 A375 or mel624 cells and treated with 0.2% L-nil for the indicated time, starting on day 3. Cisplatin was given as three i.p. injections of 2.5 mg/kg (A375) or 6 mg/kg (mel624) spaced 3 d apart, beginning on day 13 (mel624) or day 25 (A375). The numbers to the right of each curve give the fraction of surviving mice. For A375 $P < 0.001$ for CDDP + L-nil versus CDDP alone; $P = 0.009$ for CDDP + L-nil versus L-nil alone. For mel624 $P < 0.001$ for CDDP + L-nil versus CDDP alone; $P = 0.010$ for CDDP + L-nil versus L-nil alone on day 30.

although NO has been shown to suppress T cell–dependent immune responses, our immunodeficient human/mouse xenograft model is not ideal for studying effects of iNOS inhibition on tumor-mediated immunosuppression and interference with endogenous antitumor immunity.

In summary, this study clearly shows the robust antitumor effect of iNOS-selective small molecule inhibitors in a preclinical human melanoma model and their ability to synergize with conventional cytotoxic chemotherapy *in vivo*. The lack of appreciable toxicity associated with chronic L-nit treatment and its ability to enhance the efficacy of cisplatin suggest that iNOS inhibition, alone or in combination with cytotoxic chemotherapy, deserves evaluation in clinical trials for melanoma and other solid tumors. More generally, the regulation of inflammatory mediators in cancer is a promising approach to targeted cancer therapy and reversal of chemoresistance.

Disclosure of Potential Conflicts of Interest

No potential conflicts of interest were disclosed.

References

- Kundu JK, Surh Y. Inflammation: gearing the journey to cancer. *Mutat Res* 2008;659:15–30.
- Li L, Xu H. Inducible nitric oxide synthase, nitrotyrosine and apoptosis in gastric adenocarcinomas and their correlation with a poor survival. *World J Gastroenterol* 2005;11:2539–44.
- Vakkala M, et al. Inducible nitric oxide synthase expression, apoptosis, and angiogenesis in *in situ* and invasive breast carcinomas. *Clin Cancer Res* 2000;6:2408–16.
- Cianchi F, et al. Inducible Nitric Oxide Synthase Expression in Human Colorectal Cancer Correlation with Tumor Angiogenesis (ASIP); 2003.
- Brennan PA, et al. Inducible nitric oxide synthase: correlation with extracapsular spread and enhancement of tumor cell invasion in head and neck squamous cell carcinoma. *Head Neck* 2008;30:208–14.
- Pukkila MJ, et al. Inducible nitric oxide synthase expression in pharyngeal squamous cell carcinoma: relation to p53 expression, clinicopathological data, and survival. *Laryngoscope* 2002;112:1084–8.
- Albina JE, Reichner JS. Role of nitric oxide in mediation of macrophage cytotoxicity and apoptosis. *Cancer Metastasis Rev* 1998;17:39–53.
- Thomas DD, et al. Heme proteins and nitric oxide (NO): the neglected, eloquent chemistry in NO redox signaling and regulation. *Antioxid Redox Signal* 2003;5:307–17.
- Landar A, Darley-Usmar VM. Nitric oxide and cell signaling: modulation of redox tone and protein modification. *Amino Acids* 2003;25:313–21.
- Gow AJ, Farkouh CR, Munson DA, Posencheg MA, Ischiropoulos H. Biological significance of nitric oxide-mediated protein modifications. *Am J Physiol Lung Cell Mol Physiol* 2004;287:L262–8.
- Dai Fukumura SK, Jain RK. The role of nitric oxide in tumour progression. *Nat Rev Cancer* 2006;6:521.
- Ekmekcioglu S, Tang C, Grimm EA. NO news is not necessarily good news in cancer. *Curr Cancer Drug Targets* 2005;5:103–15.
- Wink DA, Ridnour LA, Hussain SP, Harris CC. The reemergence of nitric oxide and cancer. *Nitric Oxide* 2008;19:65–7.
- Azad N, et al. S-nitrosylation of Bcl-2 inhibits its ubiquitin-proteasomal degradation: a novel antiapoptotic mechanism that suppresses apoptosis. *J Biol Chem* 2006;281:34124.
- Mannick JB, et al. S-Nitrosylation of Mitochondrial Caspases: Rockefeller Univ Press; 2001.
- Bogdan C. Nitric oxide and the immune response. *Nat Immunol* 2001;2:907–16.
- American Cancer Society (2009). *Cancer Facts and Figures: 2009*.
- Massi D, et al. Inducible nitric oxide synthase expression in benign and malignant cutaneous melanocytic lesions. *J Pathol* 2001;194:194–200.
- Ekmekcioglu S, et al. Tumor iNOS predicts poor survival for stage III melanoma patients. *Int J Cancer* 2006;119:861–6.
- Ekmekcioglu S, et al. Inducible nitric oxide synthase and nitrotyrosine in human metastatic melanoma tumors correlate with poor survival. *Clin Cancer Res* 2000;6:4768–75.
- Tang C, Grimm EA. Depletion of endogenous nitric oxide enhances cisplatin-induced apoptosis in a p53-dependent manner in melanoma cell lines. *J Biol Chem* 2004;279:288–98.
- Moore WM, et al. L-N6-(1-iminoethyl)lysine: a selective inhibitor of inducible nitric oxide synthase. *J Med Chem* 1994;37:3886–8.
- Xie K, et al. Transfection with the inducible nitric oxide synthase gene suppresses tumorigenicity and abrogates metastasis by K-1735 murine melanoma cells. *J Exp Med* 1995;181:1333–43.
- Berkels R, Puroil-Schnabel S, Roesen R. A new method to measure nitrate/nitrite with a NO-sensitive electrode. *J Appl Physiol* 2001;90:317–20.
- Bryan NS, Grisham MB. Methods to detect nitric oxide and its metabolites in biological samples. *Free Radic Biol Med* 2007;43:645–57.
- Seki H, et al. Differential protective action of cytokines on radiation-induced apoptosis of peripheral lymphocyte subpopulations. *Cell Immunol* 1995;163:30–6.
- Tibes R, et al. Reverse phase protein array: validation of a novel proteomic technology and utility for analysis of primary leukemia specimens and hematopoietic stem cells. *Mol Cancer Ther* 2006;5:2512–21.
- Kozioł JA, Maxwell DA, Fukushima M, Colmerauer ME, Pilch YH. A distribution-free test for tumor-growth curve analyses with application to an animal tumor immunotherapy experiment. *Biometrics* 1981;37:383–90.
- Jenkins DC, et al. Human colon cancer cell lines show a diverse pattern of nitric oxide synthase gene expression and nitric oxide generation. *Br J Cancer* 1994;70:847–9.

Acknowledgments

We thank Dr. Nina Chinosornvatana (Department of Otolaryngology, Mount Sinai School of Medicine) for assistance in performing experiments (which contributed to Fig. 6B), Ajish George (Department of Biomedical Sciences, School of Public Health, SUNY Albany) for helpful advice regarding molecular pathway analysis, and the M.D. Anderson Small Animal Imaging Facility for the MRI analysis (supported by M.D. Anderson Cancer Center Support Grant CA016672).

Grant Support

P50 CA09349 (PP-DRP5 and PP-CDP5), University of Texas M.D. Anderson Cancer Center Specialized Programs of Research Excellence in Melanoma (E.A. Grimm, W.W. Overwijk, A.G. Sikora); NIDCD National Research Service Award Institutional Training Grant T32 D007367 (A. Gelbard, A.G. Sikora); American Head and Neck Society/American Academy of Otolaryngology Young Investigator Award (A.G. Sikora); and NCI#-CA16672 supporting the M.D. Anderson Cancer Center Characterized Cell Line Core and RPPA Core Laboratories.

This work was partially supported by VENI Grant 916.046.014 from the Netherlands Organization for Scientific Research (NWO) to W.W.O.

The costs of publication of this article were defrayed in part by the payment of page charges. This article must therefore be hereby marked advertisement in accordance with 18 U.S.C. Section 1734 solely to indicate this fact.

Received 11/25/2009; revised 01/22/2010; accepted 01/22/2010; published OnlineFirst 03/09/2010.

30. Wang G, Ji B, Wang X, Gu J. Anti-cancer effect of iNOS inhibitor and its correlation with angiogenesis in gastric cancer. *World J Gastroenterol* 2005;11:3830–3.
31. Shang Z, Li Z, Li J. *In vitro* effects of nitric oxide synthase inhibitor L-NAME on oral squamous cell carcinoma: a preliminary study. *Int J Oral Maxillofac Surg* 2006;35:539–43.
32. Madhunapantula SRV, et al. PBISe, a novel selenium-containing drug for the treatment of malignant melanoma. *Mol Cancer Ther* 2008;7:1297.
33. Malone JM, Saed GM, Diamond MP, Sokol RJ, Munkarah AR. The effects of the inhibition of inducible nitric oxide synthase on angiogenesis of epithelial ovarian cancer. *Am J Obstet Gynecol* 2006;194:1110.
34. Engels K, et al. NO signaling confers cytoprotectivity through the survivin network in ovarian carcinomas. *Cancer Res* 2008;68:5159–66.
35. Fetz V, et al. Inducible NO synthase confers chemoresistance in head and neck cancer by modulating survivin. *Int J Cancer* 2009;124:2033–41.
36. Roy HK, et al. Inducible nitric oxide synthase (iNOS) mediates the early increase of blood supply (EIBS) in colon carcinogenesis. *FEBS Lett* 2007;581:3857–62.
37. Singh RP, Agarwal R. Inducible nitric oxide synthase-vascular endothelial growth factor axis: a potential target to inhibit tumor angiogenesis by dietary agents. *Curr Cancer Drug Targets* 2007;7:475–83.
38. Pervin S, Singh R, Hernandez E, Wu G, Chaudhuri G. Nitric oxide in physiologic concentrations targets the translational machinery to increase the proliferation of human breast cancer cells: involvement of mammalian target of rapamycin/eIF4E pathway. *Cancer Res* 2007;67:289–99.
39. Hatanaka T, et al. Na⁺- and Cl⁻-coupled active transport of nitric oxide synthase inhibitors via amino acid transport system B(0,+). *J Clin Invest* 2001;107:1035–43.
40. Hansel TT, et al. A selective inhibitor of inducible nitric oxide synthase inhibits exhaled breath nitric oxide in healthy volunteers and asthmatics. *FASEB J* 2003;17:1298–300.
41. Lassen LH, Christiansen I, Iversen HK, Jansen-Olesen I, Olesen J. The effect of nitric oxide synthase inhibition on histamine induced headache and arterial dilatation in migraineurs. *Cephalalgia* 2003;23:877–86.
42. Freedman BI, et al. Design and baseline characteristics for the aminoguanidine Clinical Trial in Overt Type 2 Diabetic Nephropathy (ACTION II). *Control Clin Trials* 1999;20:493–510.
43. Karaman MW, et al. A quantitative analysis of kinase inhibitor selectivity. *Nat Biotechnol* 2008;26:127–32.

Clinical Cancer Research

Targeted Inhibition of Inducible Nitric Oxide Synthase Inhibits Growth of Human Melanoma *In vivo* and Synergizes with Chemotherapy

Andrew G. Sikora, Alexander Gelbard, Michael A. Davies, et al.

Clin Cancer Res 2010;16:1834-1844. Published OnlineFirst March 9, 2010.

Updated version	Access the most recent version of this article at: doi:10.1158/1078-0432.CCR-09-3123
Supplementary Material	Access the most recent supplemental material at: http://clincancerres.aacrjournals.org/content/suppl/2010/03/16/1078-0432.CCR-09-3123.DC1

Cited articles	This article cites 40 articles, 9 of which you can access for free at: http://clincancerres.aacrjournals.org/content/16/6/1834.full#ref-list-1
Citing articles	This article has been cited by 11 HighWire-hosted articles. Access the articles at: http://clincancerres.aacrjournals.org/content/16/6/1834.full#related-urls

E-mail alerts	Sign up to receive free email-alerts related to this article or journal.
Reprints and Subscriptions	To order reprints of this article or to subscribe to the journal, contact the AACR Publications Department at pubs@aacr.org .
Permissions	To request permission to re-use all or part of this article, use this link http://clincancerres.aacrjournals.org/content/16/6/1834 . Click on "Request Permissions" which will take you to the Copyright Clearance Center's (CCC) Rightslink site.